DOI: 10.1002/ejoc.200700419

# A Simple and Intuitive Description of C–H Bond Energies

**Amnon Stanger*[a]**

**Keywords:** DFT calculations / NBO analysis / C–H bond dissociation energies / Hybridization

Thirty-five different C–H bond dissociation energies (BDEs) of cycloalkanes and cycloalkenes, including secondary, tertiary, allyl and vinyl, of hydrocarbons, bridgeheads in bicyclic hydrocarbons, difluoro, tetrafluoro, disilyl and tetrasilyl derivatives were studied computationally. It is shown that all these BDEs can be rationalized to a large extent using the hybridization of the lobe that forms the broken C–H bond and the stabilization of the radical. This rationalization is used in a semi-quantitative manner to predict BDEs based on low-level computations of the hybridization.


## Introduction

Several attempts to understand the factors that govern C–H bond dissociation energies (BDEs, defined as the $\Delta H°$ of reaction (1) have been discussed in the last two decades.

$$R–H \rightarrow R^{\cdot} + H^{\cdot} \quad (1)$$

This topic experiences a revival, especially regarding effects that have not been considered before or are re-examined (e.g., hyperconjugation)[1] and in relation to strain in small rings.[2] The relation between strain and C–H bond energies is not clear. The literature contains several attempts to quantify strain within bond energy concepts which include, for example, bond lengths,[3] atomization energies,[4] energy density over interatomic distances[1e] and C–H bond strengthening as a stabilizing factor in cyclopropane.[5] Recently, it was shown that most of the strain in three-membered ring systems is angular strain, but the C–H bond energies rationalize the different strain in these systems.[2] In many cases the above-mentioned approaches are useful, but the details and accuracies result in the loss of the intuitive picture. Furthermore, although the MO approach has proven to be computationally more successful than VB (and hence form the basis of the above-mentioned papers) organic chemists still think in VB terms, namely resonance structures and hybridizations.[6] Since organic chemists are the main experimental users of compounds containing C–H bonds, it is desirable to formulate a general understanding and predicting power in VB terms.

An intuitive approach for the understanding of C–H bond dissociation energies in relation to strain may be based on hybridization. Usually, an $sp^3$ hybridization is assigned to tetracoordinate carbon atoms. However, unless the symmetry around the carbon is tetrahedral the hybridization cannot be $sp^3$ for all the lobes. If this argument is taken to an extreme case, e.g., cyclopropane, it is clear that the lobes forming the C–C bonds must have a p character larger than 3 (i.e., $sp^n$, where $n > 3$) as is manifested in MO terminology by the Walsh orbitals. The result is that the lobes that form the C–H bonds must have a p character smaller than 3. It is well established that bond properties highly depend on the hybridization of the carbon. For example the C–H BDEs in methane, ethylene and acetylene equal to about 105, 110.6 and 130.9 kcal mol$^{-1}$, respectively,[7] indicating that as the p character decreases the bond becomes stronger and shorter (1.0906, 1.0851 and 1.0631 Å, respectively, at B3LYP/6-311++G(d,p) level). This principle was shown also for C–C bond lengths in benzene, where changing the hybridization through the deformation of HCC bond angles localizes the C–C bonds.[8] Thus, because the hybridization changes, the C–H bond in cyclopropane should have a larger BDE than an unstrained C($sp^3$)–H bond. This is indeed so. The question that this paper tries to answer is: Can this simple principle be used for a good description of C–H bond energies and to understand the differences between different C–H bond dissociation energies?

## Methods

Gaussian 03[9] was used for the calculations. All the molecules and radicals underwent full geometry optimization within B3LYP/6-311G* theoretical level, and analytical frequencies calculations to ensure real minima ($N_{imag} = 0$) and to obtained ZPE corrections necessary for the thermodynamic correction of the total energies (enthalpies at 298 K in kcal mol$^{-1}$ are used here). The hybridizations were obtained from NBO[10] analyses of the systems under study.

[a] Schulich Faculty of Chemistry and The Lise-Meitner-Minerva Center for Computational Quantum Chemistry, Technion – Israel Institute of Technology,
Haifa 32000, Israel
Fax: +972-4-829-3944
E-mail: stanger@tx.technion.ac.il
Supporting information for this article is available on the WWW under http://www.eurjoc.org or from the author.

  

Cyclopropane, cyclobutane, cyclopentane, cyclohexane, cyclopropene, cyclobutene, hydrogen atom and the radicals resulting from the C–H cleavage of **1**–**8** were also calculated at G3.[11]

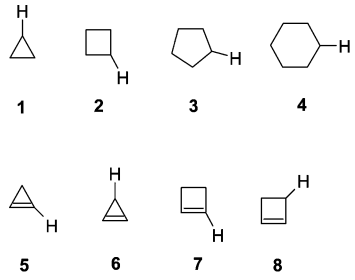


NBO is a method that (among others) allows conversion of the MO results into VB terms such as hybridization and resonance structures. However, as most MO-based methods are, its results depend on the computational level. The question is therefore how trustful are the NBO hybridizations? In order to answer this, NBO analysis was carried out for the carbon atoms bound to the hydrogen atom in **1**–**8** at eight different theoretical levels; HF/3-21G, HF/6-31G, HF/6-31G*, HF/6-311G*, HF/6-311+G*, B3LYP/6-31G*, B3LYP/6-311G* and B3LYP/6-311+G*. The absolute hybridization changes quite considerably for the different levels. For example, the hybridization of **1** changes from $sp^{2.49}$ (HF/3-21G) to $sp^{2.70}$ (HF/6-311G*), that of **5** changes from $sp^{1.52}$ (HF/6-31G) to $sp^{1.62}$ (at HF/6-311+G* and B3LYP/6-311G*). However, the linear correlations between each two computational levels are excellent. The worst correlation coefficient is 0.998 (HF/3-21G vs. B3LYP/6-311G*), the best is 1. (for HF/6-31G* vs. HF/6-31G). All the rest of the correlation coefficients are equal or larger than 0.999, most are larger than 0.9995. Thus, as long as the NBO hybridizations that are calculated at the same computational level are used for correlations with other parameters it is unimportant at which theoretical levels the values were obtained.

Can different hybridizations of tetracoordinate carbon atoms be correlated to C–C bond energies? From the limited amount of data it seems that the answer is positive. Thus, the intrinsic C–C bond energies in cyclopropane, cyclobutane and cyclohexane are 73.2, 79.1 and 87.3 kcal mol$^{-1}$, respectively,[5] whereas the C–C hybridizations of the respective C–C bonding lobes are $sp^{3.40}$, $sp^{2.86}$ and $sp^{2.53}$, respectively, at B3LYP/6-311G*.

The experimental, G3 and B3LYP/6-311G* calculated BDEs for **1**–**8** are given in Table 1.

Table 1. Bond dissociation energies [kcal mol$^{-1}$] for **1**–**8**.

| | **1** | **2** | **3** | **4** | **5** | **6** | **7** | **8** |
|---|---|---|---|---|---|---|---|---|
| Exp.[a] | 106.3 | 96.5 | 95.6 | 95.5 | 106.7 | 90.6 | 112.5 | 91.2 |
| G3 | 109.2 | 100.6 | 96.9 | 99.4 | 109.6 | 100.4 | 111.9 | 90.6 |
| B3LYP[b] | 103.6 | 94.5 | 91.1 | 93.8 | 104.4 | 95.4 | 107.2 | 86.1 |

[a] From ref.[10] [b] $\Delta H^0$ as calculated at B3LYP/6-311G* theoretical level.

A comparison between the G3 and B3LYP/6-311G* results suggests that the latter is ca. 5 kcal mol$^{-1}$ smaller than the former. However, the two correlate linearly with a correlation coefficient of 0.9969, so that the use of BDEs that are obtained at the lower level for correlations is justified. The fit between the experimental and G3 BDEs is not very good. G3 should yield energies which are within 1 kcal mol$^{-1}$ from the experimental values. Indeed, for **3**, **7** and **8** the agreement between G3 and the experimental values is very good, but for the rest of the BDEs the discrepancy is much larger – up to 9.8 kcal mol$^{-1}$ in **6**. Also, the linear correlation between the experimental and G3 BDEs is not very good ($R^2$ = 0.9116, Figure 1, a). What is the source of this discrepancy?

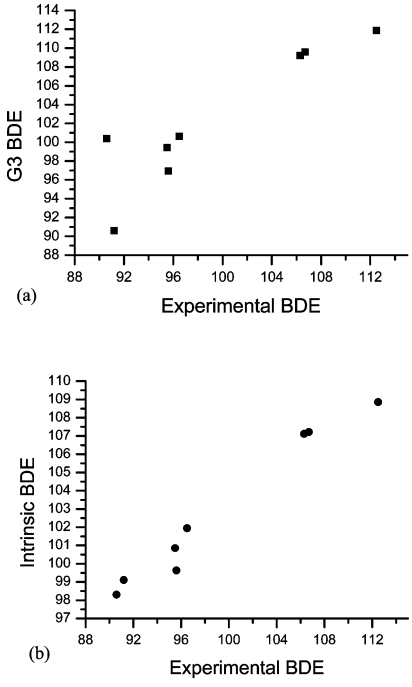


Figure 1. Plots of (a, top) experimental BDE vs. G3-calculated BDE and (b, bottom) experimental BDE vs. B3LYP/6-311G* intrinsic bond energies (scales are in kcal mol$^{-1}$).

The process of breaking a bond to form two radicals may be divided into two steps that are not measurable but can be computed.[2] The first step is the homolytic cleavage of the bond to yield two radicals, each at the same geometry they had when bound to each other. The energy associated with this process is called "intrinsic bond energy". The second step is geometrical relaxation of the radicals which releases "reorganization energy". The sum of the energies associated with these two processes (the first positive, the second negative) adds to yield the thermodynamic (and measurable) bond energy – BDE. In an attempt to understand the discrepancy between the experimental and computational results, the intrinsic BDE (as calculated at B3LYP/6-311G*) were plotted against the experimental BDEs. This plot is shown in part b of Figure 1 and suggests that the linear correlation between the experimental data and the intrinsic bond energy ($R^2$ = 0.9853) is far better that the correlation between the experimental and G3 BDEs. It is not the aim of this paper to question published experimen-

  

tal or theoretical data, but consistency requires that the correlations that are used below will use B3LYP/6-311G* (e.g., G3 through the correlation given above) BDEs rather than experimental BDEs, even if available.

## Results and Discussion

### Model Studies

In order to examine if the idea of a correlation between hybridization and BDE has any foundation model studies were carried out. A suitable model should be able to study only the desired effect(s) without the complication of other (saddle) effects that always exist in real system and may mask the main effect. Among the thirty five bonds that are studied here there are three principle types of bonds: alkyl, allyl and vinyl. The following describes how each of these bonds behaves in the models as the function of hybridization.

**Alkyl C–H bonds:** The BDEs of propane were studied as a function of the CCC bond angles ranging from 70 to 160 degrees (Scheme 1).

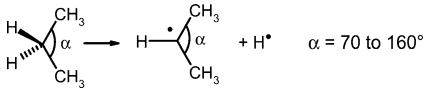


Scheme 1. Model study of BDH in propane.

The molecule and the respective radical were fully optimized except for the imposed CCC bond angle. The absolute energies of the propane and the 2-propyl radical are, of course, higher than the respective species at their optimized geometries. For example, propane molecules with CCC angles of 70 and 160 degrees are 75.6 and 38.4 kcal mol$^{-1}$ less stable than propane in its optimal geometry, respectively, and the radicals are 93.6 and 22.0 kcal mol$^{-1}$ less stable than the 2-propyl radical in its optimal geometry for the same respective angle. However, the interest here is how the hybridizations and the BDEs change as a function of the CCC bond angle.

Table 2. CCC bending angles, hybridization and BDEs of the secondary C–H bond in propane as functions of the bending angles.

| CCC angle [degrees] | $n$ of sp$^n$ | BDE [kcal mol$^{-1}$] |
|---|---|---|
| 70 | 2.23 | 111.43 |
| 75 | 2.40 | 109.51 |
| 80 | 2.57 | 107.52 |
| 85 | 2.73 | 104.89 |
| 90 | 2.89 | 102.86 |
| 95 | 3.05 | 101.45 |
| 100 | 3.20 | 99.51 |
| 105 | 3.36 | 97.64 |
| 110 | 3.51 | 95.82 |
| 115 | 3.67 | 94.06 |
| 120 | 3.84 | 92.34 |
| 125 | 4.02 | 90.68 |
| 130 | 4.20 | 88.96 |
| 135 | 4.41 | 86.53 |
| 140 | 4.65 | 84.65 |
| 145 | 4.89 | 82.78 |
| 150 | 5.16 | 80.90 |
| 155 | 5.46 | 78.99 |
| 160 | 5.79 | 77.05 |

Table 2 summarizes the results. The hybridization changes smoothly with the bond angle so that the larger the CCC bond angle is, the hybrid that binds the hydrogen that dissociates has a larger p character. Figure 2 shows the plot of the BDEs as a function of hybridization. Clearly, the correlation is not linear, but the function is smooth. A second order polynomial fit (shown in Figure 2) yields an excellent correlation coefficient of 0.9998. Thus, when all other effects are constant, the BDE can be described as a function of only the hybridization.

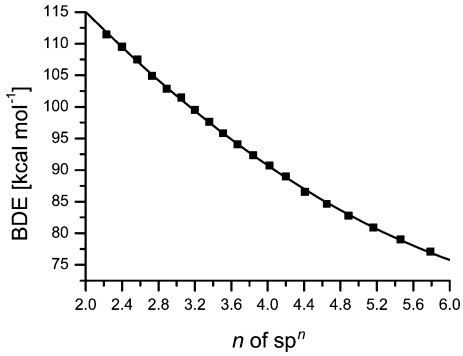


Figure 2. A plot of the BDE of propane (Scheme 1) as a function of hybridization. The line shows the second order polynomial fit.

**Allyl bonds:** The same respective study was carried out for 1-butene (Scheme 2), and the BDE was studies as a function of C(2)–C(3)–(C4) bond angle.

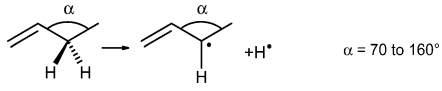


Scheme 2. Model study of BDH in 1-butene.

Table 3 summarizes the results for 1-butene. Both hybridizations of the lobes connecting the two (non-symmetrical, therefore non-equivalent) allyl hydrogen atoms change smoothly with the bond angles.

The BDEs change smoothly with hybridization, but the dependence is different from the case of propane. Whereas for small CCC angles the BDEs for propane and 2-butene are similar for the same respective hybridizations, there is an increasing difference as the bond angles become larger.

Figure 3 (a) shows the dependence of the BDEs of the allyl hydrogen atoms on hybridization, and Figure 3 (b) shows the difference between the BDEs of 1-butene and those calculated from the second-order fit parameters obtained for propane. The reason becomes clear when the geometries of the different radicals are examined (Scheme 3).

At small angles the radical lobe is almost perpendicular to the π bond (Scheme 3a), thus cannot experience any π-allyl stabilization. When the angle increases the radical lobe becomes co-planar with the π bond and experiences increasing amount of π-allyl stabilization (between 90 and 120 degrees, i.e., between sp$^3$ and sp$^4$) which becomes al-

  

Table 3. CCC bending angles, hybridization of the two allyl C–H bonds and BDEs of the allyl C–H bond in 1-butene as functions of the bending angles.

| CCC angle [degrees] | $n$ of $sp^n$ (I) | $n$ of $sp^n$ (II) | BDE [kcal mol$^{-1}$] |
|---|---|---|---|
| 70 | 2.46 | 2.42 | 108.27 |
| 75 | 2.59 | 2.54 | 107.56 |
| 80 | 2.73 | 2.67 | 105.29 |
| 85 | 2.87 | 2.80 | 102.72 |
| 90 | 3.02 | 2.93 | 100.30 |
| 95 | 3.17 | 3.06 | 94.87 |
| 100 | 3.33 | 3.19 | 90.87 |
| 105 | 3.49 | 3.33 | 87.03 |
| 110 | 3.66 | 3.46 | 83.49 |
| 115 | 3.84 | 3.61 | 80.61 |
| 120 | 4.02 | 3.76 | 77.78 |
| 125 | 4.21 | 3.93 | 75.39 |
| 130 | 4.42 | 4.11 | 73.32 |
| 135 | 4.65 | 4.31 | 71.44 |
| 140 | 4.90 | 4.53 | 70.30 |
| 145 | 5.16 | 4.77 | 68.64 |
| 150 | 5.45 | 5.04 | 66.46 |
| 155 | 5.77 | 5.35 | 64.94 |
| 160 | 6.13 | 5.7 | 63.48 |

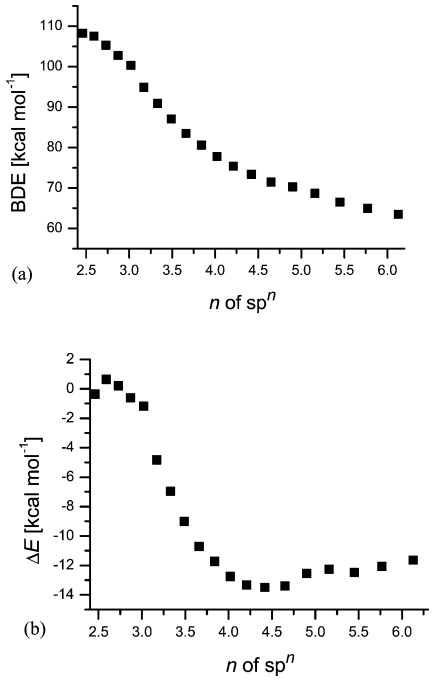


Figure 3. (a) A plot of the BDE of the allyl C–H bond in 1-butene as a function of hybridization. (b) The difference between the BDEs shown in (a) and those calculated from the bending of propane for the respective hybridizations.

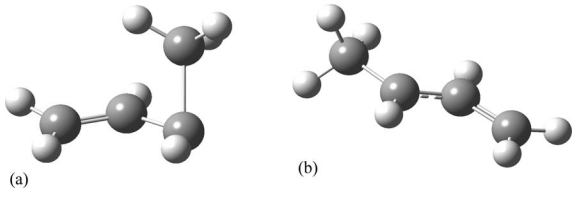


Scheme 3. Bent 1-butene. (a) $\alpha$ = 70°. (b) $\alpha$ = 120°. For the definition of α see Scheme 2.

most constant for larger bond angles. Thus, in allyl radical the BDE can be described as a second order polynom but π-allyl stabilization (which itself is a function of hybridization) should be added.

**Vinyl bonds:** For the assessment of the effect of hybridization on vinyl C–H BDEs an analogous study was undertaken for propene, calculating the hybridizations and BDEs as a function of the CCC angles (Scheme 4).

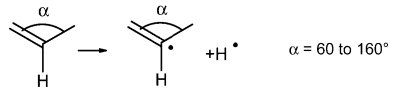


Scheme 4. Model study of BDH in propene.

Table 4 summarizes the results. As oppose to the previous models there is no smooth changes of hybridizations and BDEs as a function of the bond angles (Figure 4). At small angles the hybridization shows a minimum at 75° which corresponds to a minimum of the BDE. At larger bond angles the behavior becomes smooth for the hybridization and the BDEs. The energies of the species do not behave smoothly as well. Thus, the 75° bent propene and 2-propenyl-radical are less stable than the 60° bent species by 8.9 and 6.1 kcal mol$^{-1}$, respectively. What is then the source of the apparent stabilization (and the irregular changes in BDEs and hybridization) at small angles which are more deformed relative to the optimized geometries? The charge analysis suggests an answer. At the optimized geometries the Mulliken charges of the $CH_2$, CH and $CH_3$ moieties are –0.033, +0.037 and –0.003 electrons, respectively. It changes somewhat at 75°, being –0.008, +0.004 and –0.036, respectively. However, at 60° the charges of the $CH_2$, CH and $CH_3$ moieties are +0.064, –0.170 and +0.106 electrons, respectively.[12] Thus, at small bending angles propene is more stable on a different (more ionic) electronic surface and can-

Table 4. Hybridization and BDEs of the vinyl C–H bonds in propene as functions of the CCC bending angles.

| CCC angle [degrees] | $n$ of $sp^n$ | BDE [kcal mol$^{-1}$] |
|---|---|---|
| 60 | 3.75 | 82.37 |
| 65 | 3.67 | 83.06 |
| 70 | 1.89 | 84.81 |
| 75 | 1.27 | 79.59 |
| 80 | 1.36 | 95.90 |
| 85 | 1.46 | 105.49 |
| 90 | 1.57 | 110.87 |
| 95 | 1.70 | 113.82 |
| 100 | 1.83 | 113.83 |
| 105 | 1.96 | 112.64 |
| 110 | 2.12 | 111.68 |
| 115 | 2.30 | 109.73 |
| 120 | 2.38 | 107.65 |
| 125 | 2.70 | 105.45 |
| 130 | 2.94 | 103.08 |
| 135 | 3.20 | 100.50 |
| 140 | 3.51 | 97.65 |
| 145 | 3.87 | 94.47 |
| 150 | 4.30 | 90.87 |
| 155 | 4.82 | 86.79 |
| 160 | 5.47 | 82.18 |

  

not be compared to propene with larger CCC bond angles. More evidences for this are found in the molecular orbitals. For example, the HOMO of propene at its optimized geometry is a π-type orbital and the HOMO-1 is a σ-type orbital. In the 60° bent propene the order of these orbitals is inverted, namely, the HOMO and HOMO-1 are σ and π-type orbitals, respectively, with similar shapes on the double bond. Similar phenomena are observed for the 2-propenyl radical, although the angle where the avoided crossing between the two electronic surfaces occurs is somewhat different. However, at larger bending angles, relatively far from the avoided crossing point (since, in VB terms, the wave function near the avoided crossing contains contributions from both surfaces) the dependence of the BDEs on the hybridizations should be similar to that observed for propane. Indeed, the plot of the hybridization as a function of bending angles is smooth (Figure 5, a) and the plot of the BDEs as a function of the hybridization (Figure 5, b) for bending angles between 100–170° yields an excellent correlation for a second order polynomial fit (correlation coefficient 0.9995).

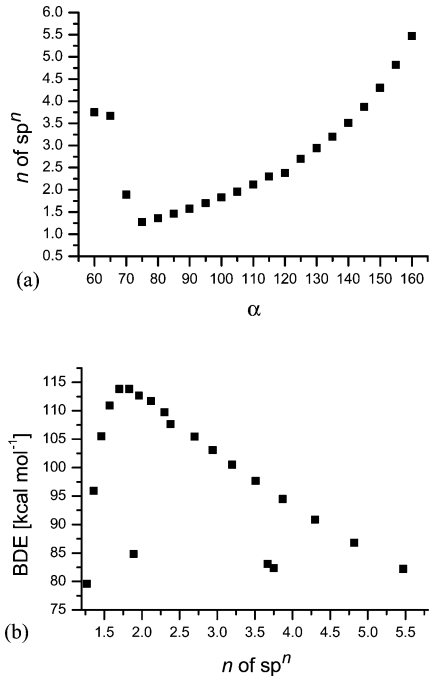


Figure 4. (a) A plot of the hybridization as a function of the bending angle in propene (Scheme 3). (b) A plot of the BDEs in bent propene (Scheme 3) as a function of hybridization.

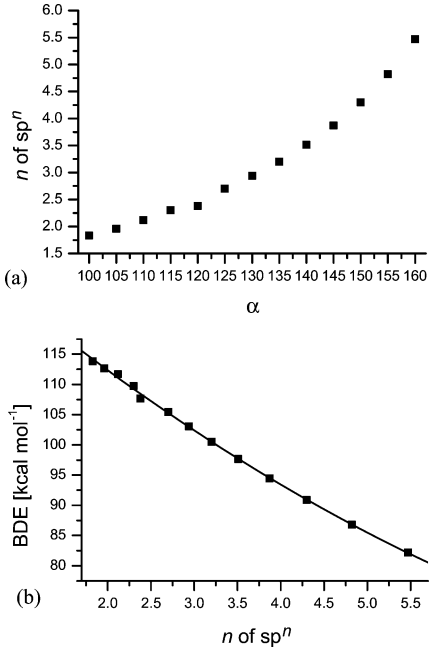


Figure 5. (a) A plot of the hybridization as a function of larger bending angle in propene (Scheme 3). (b) A plot of the BDEs in bent propene (Scheme 3) for bending angles of 100–170° as a function of hybridization including best fit second order polynomial line.

## Analysis of the BDEs of 1–35

The model studies were carried on imposed bond angles species and therefore they should better correspond to intrinsic BDEs. These studies also showed that each type of C–H bond (i.e., alkyl, allyl and vinyl) should be treated separately. The following analysis will thus concentrate on intrinsic BDEs for each of the different type of bonds. Thirty five intrinsic BDEs and BDEs were calculated. In order to be able to draw general conclusions the studied compounds contain three to six membered rings and bicyclic systems that have the three types of C–H bonds: alkyl, allyl and vinyl. Furthermore, fluorinated and silylated compounds are included. These substituents have large effects on the curvature of the bonds (and thus on hybridization), and therefore, if they fit into the approach that is considered here, strengthen the conclusion.[13]

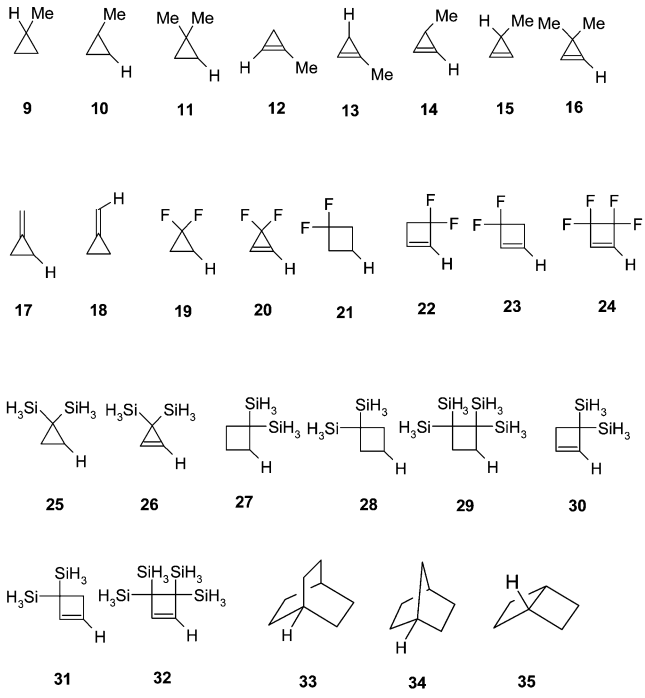


  

**Alkyl C–H bonds:** Figure 6 shows all the intrinsic BDEs of the alkyl bonds as a function of hybridization.

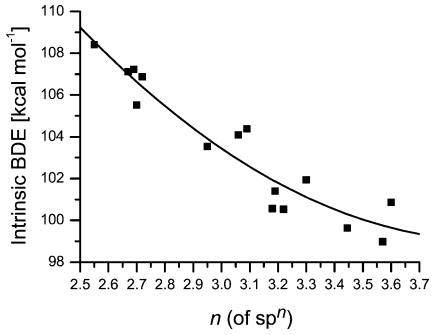


Figure 6. Alkyl intrinsic BDEs as a function of hybridization. The line indicates the second order polynomial fit.

Compound **35** is not included and treated as a vinyl bond. The reason is that the central C–C bond is composed of two $sp^{3.58}$ lobes, making the bridgehead carbon atoms more similar to tricoordinate carbon atom than to a tetracoordinate one. The correlation coefficient for a second order polynomial fit between the hybridization and the intrinsic C–H BDEs is 0.951. Considering the wide range of compounds that were studied (different ring sizes, fluoro and silyl substituents) and the fact that the deviation from the average line is $\leq 1$ kcal mol$^{-1}$ the correlation is satisfactory to prove the point.

**Allyl bonds:** Figure 7 (a) shows a plot of the allyl intrinsic BDHs as a function of the hybridization and the assignment of each point on the graph.

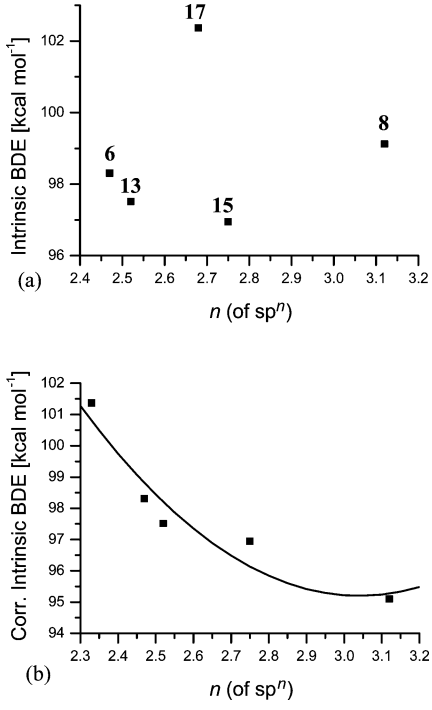


Figure 7. Allyl intrinsic BDHs as a function of hybridizations. (a) Crude data. (b) After applying allyl and hybridization corrections.

As shown above, an hybridization correction for the π-allyl stabilization should be implemented. In **6**, **13** and **15** the hybridization of the carbons at the C–H bonds are 2.47–2.75, thus (according to the model study, Figure 3, b) require no correction. However, the hybridization in **8** is 3.12. A crude estimation of the allyl stabilization is thus 5 kcal mol$^{-1}$ (Figure 3, b). Examination of the hybridizations of the C–H bonds and the radicals at the same geometries of the respective hydrocarbons suggest that they are almost unchanged except that of **17** which changes from $sp^{2.33}$ in the hydrocarbon to $sp^{2.68}$ at the radical. Figure 6 (b) shows the allyl intrinsic BDHs after applying the allyl stabilization and hybridization change to **8** and **17**, respectively together with the second order polynomial fit with a correlation coefficient of 0.9578. The correlation is far from being perfect, but comparing parts a and b of Figure 7 and considering the crude nature of the correction applied it is significantly improved. Thus, it can be concluded that also in allyl C–H bonds the intrinsic BDHs depend on hybridization.

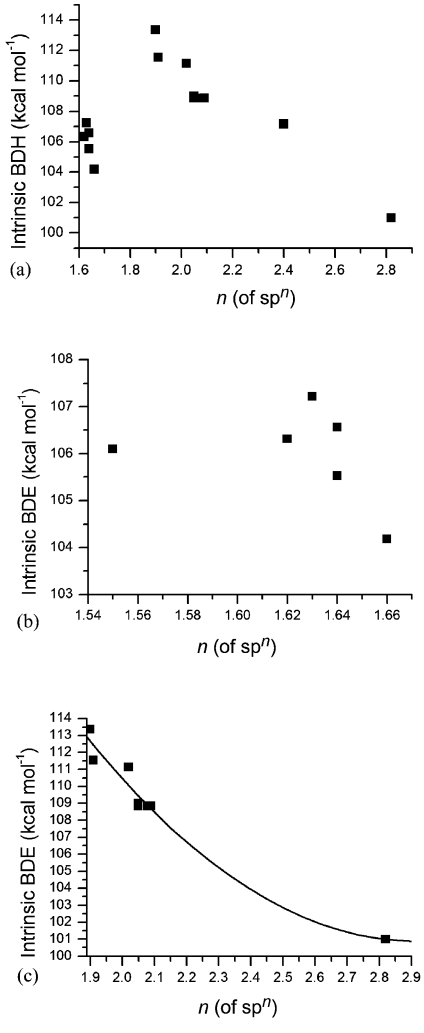


Figure 8. Vinyl intrinsic BDEs as function of hybridizations. (a) All the studies bond. (b) The group with smaller p contribution. (c) The group with larger p contribution.

  

**Vinyl bonds:** Figure 8 (a) shows a plot of the vinyl BDHs (including that of **35**) as a function of hybridization. Clearly, there are two groups of BDHs. One with a small p contribution of ca. 1.6 to 1.7, and the second with a p contribution larger than 1.8. This is in accordance to the model study of the bent propene (see above) which suggests that at small bending angles (thus, smaller p contribution in the hybrid that binds the hydrogen atom) the system lies on a different potential surface than that of larger bending angles. Hence, the two groups should be analyzed separately. Figure 8 (b) shows the dependence of the smaller *p*-containing hybrids intrinsic BDEs as a function of hybridization. Although a trend can be observed (except for **20**) a good fit is not expected. According to the model study those hybridizations are close to the avoided-crossing point of the two electronic surfaces, thus containing contributions from both in their wave functions. The hybridization and intrinsic BDE of **20** does not even fit with the trend observed for the other systems. This may be due to the combination of the effect of F on the hybridization together with its strong electron withdrawing character, suggesting that this specific system may lie on a different electronic surface. The group of vinyl C–H bonds where the lobes on the carbon atoms are $sp \geq 1.9$-hybridized shows the expected second order polynomial fit with a correlation coefficient of 0.9837 (Figure 8, c).

**Reorganization energies:** So far, it has been demonstrated that the intrinsic C–H bond dissociation energies can be understood on the basis of hybridization. However, the thermodynamic BDE contains also the relaxation energy (also called reorganization energy) which is the difference of energy between the radical at the hydrocarbon geometry and in its optimized geometry.

The first noted difference is between the reorganization energies of three-membered rings systems and larger systems. Thus, whereas the reorganization energies for cyclobutyl, cyclopentyl and cyclohexyl radicals are 7.4, 8.5 and 7.0 kcal mol$^{-1}$ respectively, it is only 3.5 kcal mol$^{-1}$ for cyclopropyl radical. Another example is the difference between the reorganization energy of allyl radicals resulting from **6** (2.9 kcal mol$^{-1}$) and **8** (13.0 kcal mol$^{-1}$). The geometries of the radicals can explain this. The radicals resulting from the three-membered rings are pyramidal, whereas those resulting from larger rings are planar. Thus, structurally the three-membered rings radicals are more similar than the larger rings radicals to the respective hydrocarbons, namely, undergo less structural reorganization. The planar geometry of the radicals of the rings larger than four allows stabilization by hyperconjugation (in the alkyl radicals) and π-allyl delocalization (in the allyl radicals) which is minimal for the three-membered rings radicals. This implies that the difference in electronic conjugation between cyclopropyl-based radical and the respective hydrocarbons is smaller than the respective difference in larger ring systems.

NICS-scan[14] (Figure 9) of cyclopropane cyclopropene, cyclobutane, cyclobutene and their radicals shows this effect.

The two three-membered rings show a NICS-scan which is very similar to that of their radicals, indicating similar cyclic conjugation in the hydrocarbons and the radicals. The four-membered rings show very different NICS scans from their radicals, indicating a different cyclic conjugation within each couple. Thus, NICS scan, although developed for the study of cyclic conjugated π system can serve as a qualitative measure for reorganization by comparing the plots of the radical with the respective hydrocarbon.

It was found that the reorganization energies of the thirty five radicals that were studies here can be divided into four groups. All three-membered rings radicals except **17** (which

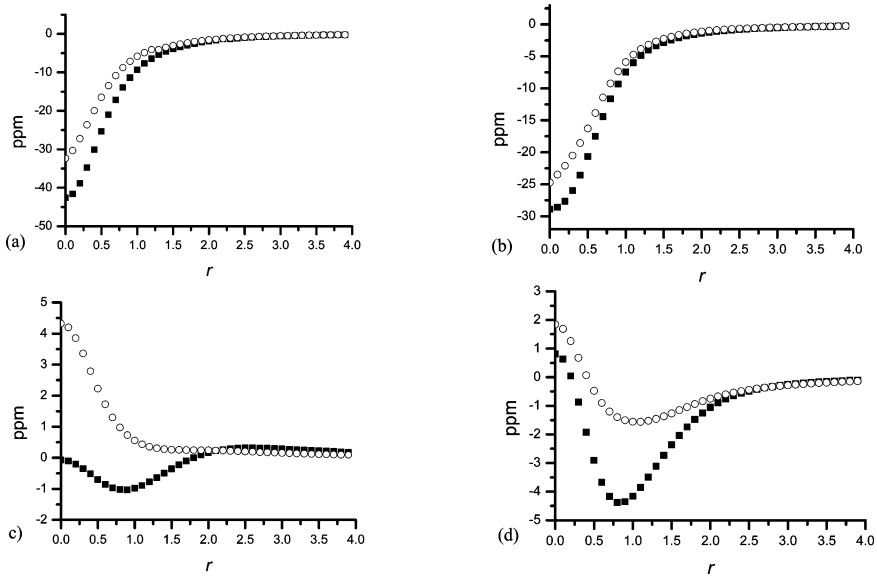


Figure 9. NICS values as a function of distance from the molecular planes of hydrocarbons (■) and their radicals (○). (a) Cyclopropane and cyclopropyl radical. (b) Cyclopropene and 3-cyclopropenyl radical. (c) Cyclobutane and cyclobutyl radical. (d) Cyclobutene and 3-cyclobutenyl radical.

  

Table 5. Hybridizations, predicted B3LYP/6-311G* intrinsic BDEs and BDEs, predicted and calculated G3 and G3MP2B3 BDEs for **36** and **37**. The error for the predicted BDEs is $\pm 2\sigma$ of the relaxation energies.

| | **36** | **36** | **37** | **37** |
|---|---|---|---|---|
| HF/3-21G hybridization | | 2.68 | | 2.12 |
| B3LYP/6-311G* hybridization | 2.36 | 2.94[c] | 2.35 | 2.29[c] |
| Predicted intrinsic BDE B3LYP/6-311G* [a] | 101.0 | 102.5 | 108.7 | 109.3 |
| Predicted intrinsic BDE B3LYP/6-311G* [b] | 102.9 | 104.0 | 107.0 | 107.0 |
| Predicted BDE B3LYP/6-311G* [a] | 92.8 ± 2.0 | 94.3 ± 2.0 | 107.2 ± 0.5 | 107.8 ± 0.5 |
| Predicted BDE B3LYP/6-311G* [b] | 94.7 ± 2.0 | 95.8 ± 2.0 | 105.4 ± 0.5 | 105.2 ± 0.5 |
| Predicted G3[a] | 98.1 ± 2.0 | 99.6 ± 2.0 | 112.5 ± 0.5 | 113.1 ± 0.5 |
| Predicted G3[b] | 100.0 ± 2.0 | 101.1 ± 2.0 | 110.7 ± 0.5 | 110.8 ± 0.5 |
| G3 BDE | 100.3 | 100.3 | 113.9 | 113.9 |
| G3MP2B3 BDE | 99.6 | 99.6 | 113.6 | 113.6 |

[a] From the model studies correlations; see Figure 2 and Figure 5 (b) for **36** and **37**, respectively. [b] From the correlations of the respective molecules; see Figure 6 and part c of Figure 8 for **36** and **37**, respectively. [c] Calculated from the linear correlations between NBO hybridizations at different computational levels.

forms an almost planar allyl radical), including alkyl, allyl and vinyl radicals have a reorganization energy of $3.32 \pm 0.47$ kcal mol$^{-1}$ (for sixteen radicals).[15] Cyclic alkyl radicals (seven radicals) and the three bicyclic radical have reorganization energies of $8.19 \pm 1.03$ and $2.33 \pm 0.31$ kcal mol$^{-1}$, respectively, and the cyclic vinyl radical (excluding cyclopropenyl, seven radicals) have a reorganization energies of $1.57 \pm 0.29$ kcal mol$^{-1}$. The allyl radicals **8** and **17** have reorganization energies of 13.0 and 10.4 kcal mol$^{-1}$, respectively.

**Semi-quantitative predictions:** So far it has been shown that a second order polynomial fit describes the intrinsic BDE as a function of hybridization, with the limitations of adding π-allyl stabilization for allyl radicals and crossing between different electronic surfaces for vinyl radicals. Reorganization energies are grouped according to the types of radicals. The question that is addressed here is if the correlations presented above (for the numerical quantities see Supporting Information) can be utilized for predicting BDEs. Of course, due to the nature of the analysis that is used in this paper, which emphasizes the conceptual aspect rather than the accuracy, it is not expected that the approach will yield exact numbers. However, the approach can become useful if it has some predicting power.

Two systems, **36** and **37**, were arbitrarily chosen to study this point. The molecules have been optimized at B3LYP/6-311G* theoretical level and underwent NBO analysis to obtain the hybridization. Optimization and NBO analysis was also carried out at HF/3-21G theoretical level.[16] The hybridizations that were obtained were used to evaluate intrinsic BDEs using the parameters obtained in the second order polynomial fits of the respective models and respective molecules of **1**–**35**. Reorganization energies were added and the correlation between G3 and B3LYP/6-311G* was used for predicting BDEs. These results (Table 5) are compared to G3[11] and G3MP2B3[17] results. Table 5 summarizes the results.

Without going into detailed analysis it seems that it is enough to carry out short calculations at HF/3-21G for obtaining quite reliable bond dissociation energies. It seems that the model correlation (Figure 6) performs better than the actual molecules correlation (Figure 8, c) for **37**. This may be due to the fact that the latter correlation is based on four-membered rings systems which may be still contaminated by another electronic surface. However, even in these worst cases the predicted BDE is only in 2.4–2.7 kcal mol$^{-1}$ from the G3 energies. Thus, it seems that the correlation between BDEs and hybridization can be used not only in a conceptual way but also to easily predict BDEs in a quantitative (or, at least semi-quantitative) way.

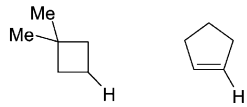


**36** **37**

## Summary and Conclusions

Models for three types of C–H bonds – alkyl, allyl and vinyl – were studied. It was shown that a second order polynomial function can describe the relation between the hybrid that bind the hydrogen atom and the intrinsic bond energy. In allyl C–H bonds the allyl stabilization of the radical (which itself is a different function of hybridization) at its non-relaxed geometry should be considered. For vinyl C–H bonds it was found that a transition between two electronic surfaces occurs. However, when far from the avoided-crossing point a good second order polynomial fit between hybridizations and intrinsic BDEs is obtained. These finding were applied for the analysis of thirty five C–H intrinsic bond dissociation energies. The relaxation energies were found to be specific for families of similar radicals due to the very large differences in the reorganization energies. In conclusion, intrinsic BDHs can be conceptually understood as functions of hybridizations. It was also shown that a calculation of hybridization even at a low computational level is enough to predict bond dissociation energies in reason-

  

able accuracies through the correlations discussed in the paper. Thus, the conceptual dependence of BDE on hybridization can also be used in a semi-quantitative way.

**Supporting Information** (see also the footnote on the first page of this article): Correlations and hybridizations at different theoretical levels.

## Acknowledgments

The Niedersaches Stiftung is acknowledged for financial support.

[1] a) K. U. Ingold, G. A. DiLabio, *Org. Lett.* **2006**, *8*, 5923; b) S. Gronert, *J. Org. Chem.* **2006**, *71*, 1209; c) M. Mitoraj, H. Zhu, A. Michalak, T. Ziegler, *J. Org. Chem.* **2006**, *71*, 9208. See also:; d) A. Kovács, C. Esterhuysen, G. Frenking, *Chem. Eur. J.* **2005**, *11*, 1813; e) R. F. W. Bader, *Chem. Eur. J.* **2006**, *12*, 7569; f) G. Frenking, C. Esterhuysen, A. Kovacs, *Chem. Eur. J.* **2006**, *12*, 7573.
[2] R. D. Bach, O. Dmitrenko, *J. Am. Chem. Soc.* **2004**, *126*, 4444.
[3] T. M. Krygowski, A. Ciesielski, C. W. Bird, A. Kotschy, *J. Chem. Inf. Comput. Sci.* **1995**, *35*, 203.
[4] S. Grimme, *J. Am. Chem. Soc.* **1996**, *118*, 1529.
[5] K. Exner, P. v. R. Schleyer, *J. Phys. Chem. A* **2001**, *105*, 3407.
[6] See, for example: S. Shaik, D. Danovich, B. Silvi, D. L. Lauvergnat, P. C. Hiberty, *Chem. Eur. J.* **2005**, *111*, 6358.
[7] Data taken from NIST Chemistry WebBook, see http://webbook.nist.gov/chemistry.
[8] A. Stanger, *J. Am. Chem. Soc.* **1991**, *113*, 8277.
[9] *Gaussian 03*, Revision B.05, M. J. Frisch, G. W. Trucks, H. B. Schlegel, G. E. Scuseria, M. A. Robb, J. R. Cheeseman, J. A. Montgomery Jr, T. Vreven, K. N. Kudin, J. C. Burant, J. M. Millam, S. S. Iyengar, J. Tomasi, V. Barone, B. Mennucci, M. Cossi, G. Scalmani, N. Rega, G. A. Petersson, H. Nakatsuji, M. Hada, M. Ehara, K. Toyota, R. Fukuda, J. Hasegawa, M. Ishida, T. Nakajima, Y. Honda, O. Kitao, H. Nakai, M. Klene, X. Li, J. E. Knox, H. P. Hratchian, J. B. Cross, V. Bakken, C. Adamo, J. Jaramillo, R. Gomperts, R. E. Stratmann, O. Yazyev, A. J. Austin, R. Cammi, C. Pomelli, J. W. Ochterski, P. Y. Ayala, K. Morokuma, G. A. Voth, P. Salvador, J. J. Dannenberg, V. G. Zakrzewski, S. Dapprich, A. D. Daniels, M. C. Strain, O. Farkas, D. K. Malick, A. D. Rabuck, K. Raghavachari, J. B. Foresman, J. V. Ortiz, Q. Cui, A. G. Baboul, S. Clifford, J. Cioslowski, B. B. Stefanov, G. Liu, A. Liashenko, P. Piskorz, I. Komaromi, R. L. Martin, D. J. Fox, T. Keith, M. A. Al-Laham, C. Y. Peng, A. Nanayakkara, M. Challacombe, P. M. W. Gill, B. Johnson, W. Chen, M. W. Wong, C. Gonzalez, J. A. Pople, Gaussian, Inc.; Wallingford CT, **2004**.
[10] Gaussian NBO (Natural Bond Orbitals) Version 3.1 was used. See A. E. Reed, L. A. Curtiss, F. Weinhold, *Chem. Rev.* **1988**, *88*, 899 and references cited therein.
[11] L. A. Curtiss, K. Raghavachari, P. C. Redfem, V. Rassolov, J. A. Pople, *J. Chem. Phys.* **1998**, *109*, 7764.
[12] NBO charges, although different from Mulliken charges show the same trend. Thus, for the optimized propene, the 75 and 90 degrees bent propenes the charges of the $CH_2$, CH and $CH_3$ moieties are: –0.01797, +0.01238, +0.0056; –0.004535, +0.05528, –0.00992; –0.00065, –0.1559, +0.15656.
[13] Fluorine-containing compounds have been shown to be problematic for calculations (see, for example, H. Wei, D. A. Hrovat, W. R. Dolbier, B. E. Smart Jr, W. T. Borden, *Angew. Chem. Int. Ed.* **2007**, *46*, 2666 and references cited therein). Therefore, if fluorine containing compounds are well handled within a given approach it proves this approach to be more general.
[14] Usually NICS is used in conjugated cyclic systems. However, NICS scan (A. Stanger, *J. Org. Chem.* **2006**, *71*, 883) that measures ring currents can be used for observing these differences.
[15] Reported are the average values $\pm\sigma$.
[16] CPU time on a PC with Windows XP™ as operating system, using the Windows version of G03 and a starting geometry of GaussView was 76 and 24 seconds for **36** and **37**, respectively, for geometry optimization and NBO analysis.
[17] a) L. A. Curtiss, P. C. Redfern, K. Raghavachari, V. Rassolov, J. A. Pople, *J. Chem. Phys.* **1999**, *110*, 4703; b) A. G. Baboul, L. A. Curtiss, P. C. Redfern, K. Raghavachari, *J. Chem. Phys.* **1999**, *110*, 7650.

Received: May 9, 2007
Published Online: September 25, 2007

  